Report on a problem studied at the UK Mathematics-in-Medicine Study Group Imperial College 2009
< http://www.maths-in-medicine.org/uk/2009/neurons-aging/ >

Measuring vesicular release from neurons

Problem Presenter
Danny O'Hare (Imperial College London)

Participants
Christopher Bell (Imperial College London),
Andrea Bonfiglio (Università degli studi di Genova),
Isaac Chenchiah (University of Bristol),
Chris Breward (University of Oxford),
Zofia Jones (University of Nottingham),
Julia Meskauskas (University of L'Aquila),
Shailesh Naire (Keele University),
Sevil Payvandi (Imperial College London),
Da-Lun Tseng (University of Oxford),
Robert Whittaker (University of Oxford),
Konstantinos Zygalakis (University of Oxford)

March 15, 2010

1 Introduction

Connections between neurons in the brain are primarily chemical, across a specialised structure called the synapse. At the synapse, vesicles containing neurotransmitter fuse with the cell membrane and release their contents into the synaptic cleft. A cartoon showing this process is pictured in Figure 1. Wightman et al. [1] suggest that vesicles may not always release their entire cargo of neurotransmitter, but sometimes may only release part. The transmitter molecules (typically 10,000-100,000 molecules per vesicle in human brains) diffuse across the synaptic cleft (around $200\times\ 10^{-9}$m) where some of them engage with receptors triggering another wave of activity in the post synaptic cell. Any remaining neurotransmitter needs to be taken back up by membrane-bound transporter proteins so they can be broken down or repackaged. It is of interest experimentally to measure how this process changes with age or drugs. For example, among other things, the experimentalists would like to understand how aging or drugs affect the concentration of neurotransmitter released from the vesicles and whether the rate of re-uptake changes.

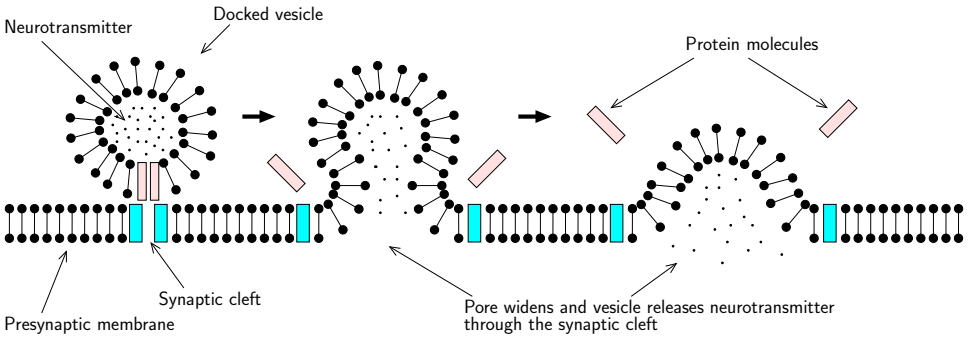

Figure 1: Cartoon showing how the vesicle docks onto the presynaptic membrane and releases its cargo of neurotransmitter through the synaptic cleft.

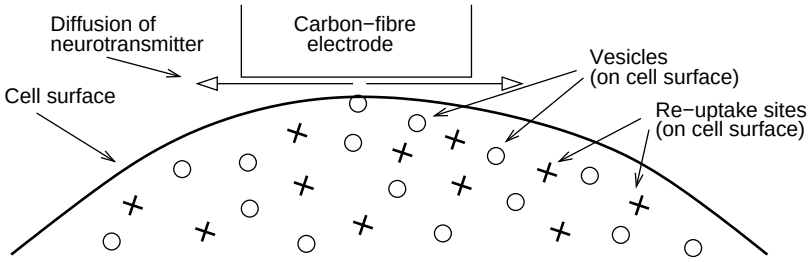

Figure 2: Experimental set-up showing vesicles and re-uptake sites distributed discretely across the cell surface.

The release of the neurotransmitter molecules can be detected using microelectrodes, with a typical experimental set-up as shown in Figure 2, cf. [2, 3, 4] and [5] (where the use of nanoelectrodes for even greater spatial resolution is discussed). Experiments have been performed by Dr O'Hare's group on the central nervous system of the pond snail, *Lymnaea stagnalis*. The distance of electrode from pre-synaptic membrane is typically around 200×10^{-9}m, and the diameter of the electrode disc is around 7×10^{-6}m. The neurotransmitter molecules are oxidised electrochemically at the surface of a small carbon fibre electrode at a sufficient rate that the surface concentration at the electrode is zero. This results in a diffusion-limited current which gives an instantaneous measurement of the rate of oxidation. A typical current profile detected from the brain of a normal young snail is shown in Figure 3, taken from data provided by Dr. O'Hare. This current has been measured over a period of 50 seconds. The background noise is about 5pA and the spikes correspond to neurotransmitter release. The spike marked A is magnified in Figure 4. Sometimes a foot is observed at the start of the current profile, [3, 4], due to a two-stage release process, but we do not consider such events in this report. The transmitter concentration rises very rapidly, then falls away, due to:

- diffusion away (diffusion coefficient of neurotransmitter of the order of $10^{-10}\mathrm{m}^2\mathrm{s}^{-1}$);
- re-uptake by the cell;
- diffusion-limited consumption by the microelectrode (the current tracks this consumption).

To obtain answers to the questions posed by the experimentalists, one would like to be able to deduce quantities such as the total concentration released from the vesicle and the rate of re-uptake from the current profile. To facilitate this, one needs a theoretical model.

Mostly only one vesicle at a time is detected using these microelectrodes and the release takes place rapidly, so it is appropriate to model the neurotransmitter release as an instantaneous point release from a boundary. Wightman et al. [2] use a random walk simulation to model the diffusional dispersion of this release, while Rabie et al. [6] use Monte Carlo methods. Parker, [7], models the initial release as a Dirac δ-function, and the subsequent dispersion using the diffusion equation. In §2, using a similar model to Parker, we derive a simple 1D diffusion model for the process, assuming uniform re-uptake across the cell membrane with constant mass transfer coefficient k. In §3, we show how the model may be solved in the form of an infinite series to provide current profiles similar to that in Figure 4. At long times, the leading current decays exponentially with a time-scale dependent on the ratio of the reuptake rate to the diffusion coefficient. At small times,

however, the series solution converges very slowly and is impractical computationally. In this range, it is better to exploit the small time parameter to derive an asymptotic solution, and we find this solution in §4.

As indicated in Figure 2, the re-uptake of the neurotransmitter does not take place uniformly across the membrane, but actually at discrete sites on the membrane. We address this problem analytically in §5 and numerically in §6. In §5, we consider the scenario when there are very many small perfectly absorbing re-uptake sites distributed evenly across the membrane, such that the size of the site and the distance between them is small when compared to the distance between the membrane and the electode. In this case the non-uniformity of the membrane will only affect a small boundary layer close to the membrane, and it is possible to derive the effective uniform mass transfer coefficient from the solution in the boundary layer. In §6, we perform numerical simulations to show how the current detected at the electrode is affected by the presence of a single re-uptake site at a distance d from the original release site. The current detected is critically dependent on both the distance d, the rate of re-uptake k and the diffusion coefficient of the neurotransmitter.

Finally in §7, we conclude and make some suggestions for future work.

2 Modelling

We assume that the pre synaptic membrane is at $z^* = b$, and the electrode surface at $z^* = a$, where $b > a$. We can model the membrane and the electrode as two planes since the distance between the electrode and the membrane surface (200×10^{-9}m) is much smaller than the diameter of the electrode (7×10^{-6}m). We use cylindrical polar coordinates and denote the concentration of neurotransmitter by $C^*(r^*, \theta, z^*, t^*)$, where the $*$'s indicate dimensional variables. For $a < z^* < b$, it satisfies the 3D diffusion equation:

$$\frac{\partial C^*}{\partial t^*} = D\left(\frac{\partial^2 C^*}{\partial z^{*2}} + \hat{\nabla}^2 C^*\right). \tag{1}$$

Here $\hat{\nabla}^2$ is the 2D Laplacian in r^* and θ, and D is the diffusion coefficient of the neurotransmitter. At the electrode surface the reaction of the neurotransmitter is diffusion limited so that the concentration is zero there, giving the boundary condition:

$$C^*(r^*, \theta, a, t^*) = 0. \tag{2}$$

On the surface of the presynaptic membrane, we assume that the flux through the discrete re-uptake sites may be modelled as a homogeneous flux across the whole boundary, modelled by a mass transfer coefficient, k, so that the re-uptake is proportional to the concentration at the boundary:

$$-D\frac{\partial C^*}{\partial z^*}(r^*, \theta, b, t^*) = kC^*(r^*, \theta, b, t^*). \tag{3}$$

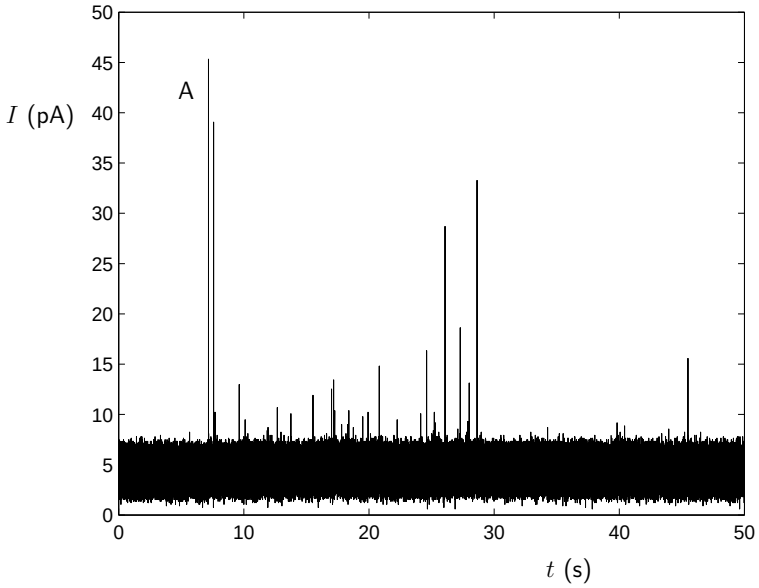

Figure 3: Current produced over a 50 second interval from a normal young snail, showing spikes due to releases of neurotransmitter. The spike A is magnified in Figure 4 below.

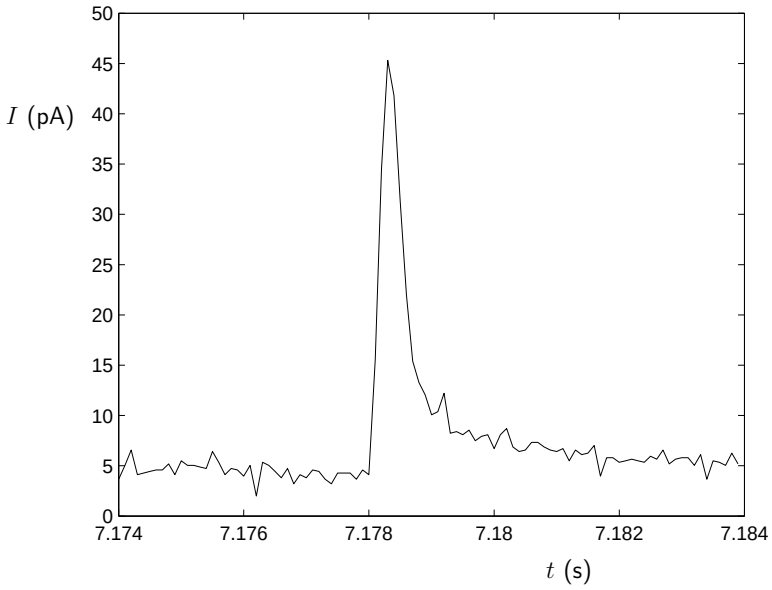

Figure 4: Magnification of the spike A in Figure 3 above due to a single release of neurotransmitter.

Therefore $k = 0$ corresponds to no re-uptake, and $k = \infty$ corresponds to infinite uptake. As $r^* \to \infty$, we assume that none of the neurotransmitter diffuses beyond the edges of the electrode; either it is re-uptaken by the membrane, or it oxidises at the electrode. This gives the boundary condition:

$$C^*(r^*, \theta, z^*, t^*) \to 0, \text{ as } r^* \to \infty. \tag{4}$$

Following the analysis of Parker [7], we assume that the initial release of the neurotransmitter can be modelled as point source at $(r^* = 0, z^* = b)$ using the Dirac δ-function, so that

$$C^*(r^*, \theta, z^*, 0) = 2C_0 \left(\frac{\delta(z^* - b)\delta(r^*)}{\pi r^*} \right). \tag{5}$$

Here C_0 mol m^{-3} is the initial concentration within the vesicle, and the factor of 2 is so that

$$\int_a^b \int_0^{2\pi} \int_0^{\infty} C^*(r^*, \theta, z^*, 0)\, r^*\, dr^* d\theta dz^* = C_0. \tag{6}$$

The current I^* is given by

$$I^*(t^*) = nFD \int_0^{2\pi} \int_0^{\infty} \frac{\partial C^*}{\partial z^*}(r^*, \theta, a, t^*) r^* dr^* d\theta, \tag{7}$$

where F is Faraday's constant and n is the number of electrons exchanged at the electrode surface in the oxidation reaction.

2.1 Non-dimensionalisation

We non-dimensionalise the problem using the following scalings:

$$C^* = C_0 \hat{C}, \quad z^* = a + (b - a)z, \quad r^* = (b - a)r, \quad t^* = \frac{(b - a)^2}{D} t, \tag{8}$$

$$I^* = nFC_0 D(b - a)I, \tag{9}$$

The governing equation (1) becomes

$$\frac{\partial \hat{C}}{\partial t} = \frac{\partial^2 \hat{C}}{\partial z^2} + \hat{\nabla}^2 \hat{C}, \tag{10}$$

and the boundary and initial conditions (2) to (5) become

$$\hat{C}(r, \theta, 0, t) = 0, \tag{11}$$

$$-\frac{\partial \hat{C}}{\partial z}(r, \theta, 1, t) = \kappa \hat{C}(r, \theta, 1, t), \tag{12}$$

$$\hat{C}(r, \theta, z, t) \to 0, \text{ as } r \to \infty, \tag{13}$$

$$\hat{C}(r, \theta, z, 0) = 2 \left(\frac{\delta(z - 1)\delta(r)}{\pi r} \right). \tag{14}$$

In (12), the non-dimensional mass transfer coefficient is given by

$$\kappa = \frac{(b-a)k}{D}. \tag{15}$$

The non-dimensional current becomes

$$I(t) = \int_0^{2\pi} \int_0^{\infty} \frac{\partial \hat{C}}{\partial z}(r, \theta, 0, t) r dr d\theta. \tag{16}$$

2.2 Simplification of the model to the 1D dimensional diffusion equation

Since we are assuming that the mass transfer coefficient κ is a constant, the boundary conditions do not have any dependence on r or θ, and since the initial condition is separable in r and z, we see that we may integrate out any r or θ dependence in the problem. Integrating (10) with respect to r and θ over a circle of radius R, called Γ_R, at any z and applying the divergence theorem gives

$$\frac{\partial}{\partial t} \int_0^{2\pi} \int_0^{R} \hat{C} r dr d\theta = \frac{\partial^2}{\partial z^2} \int_0^{2\pi} \int_0^{R} \hat{C} r dr d\theta + \int_{\Gamma_R} \hat{\nabla} \hat{C} \cdot \hat{n} dl. \tag{17}$$

If we let $R \to \infty$ in (17) and define

$$C(z,t) = \int_0^{2\pi} \int_0^{\infty} \hat{C}(r, \theta, z, t) r dr d\theta, \tag{18}$$

then we find that $C(z,t)$ satisfies the 1D diffusion equation:

$$\frac{\partial C}{\partial t} = \frac{\partial^2 C}{\partial z^2}. \tag{19}$$

The last term in (17) tends to zero as the boundary condition (13) implies that $\partial \hat{C}/\partial r \to 0$ as $r \to \infty$. The equivalent boundary and initial conditions are:

$$C(0,t) = 0, \tag{20}$$

$$-\frac{\partial C}{\partial z}(1,t) = \kappa C(1,t), \tag{21}$$

$$C(z,0) = 2\delta(z-1), \tag{22}$$

The non-dimensional current (16) becomes

$$I(t) = \frac{\partial C}{\partial z}(0,t). \tag{23}$$

3 Solution of the 1D diffusion model

Using separation of variables and the boundary conditions (20) and (21), we find that

$$C(z,t) = \sum_{i=0}^{\infty} B_i \sin(\lambda_i z) e^{-\lambda_i^2 t}, \tag{24}$$

where the λ_i are the roots of:

$$\tan \lambda_i = -\frac{\lambda_i}{\kappa}, \tag{25}$$

and the B_i are constants determined from the initial condition (22) to be

$$B_i = \frac{\sin \lambda_i}{\frac{1}{2} - \frac{1}{4\lambda_i} \sin 2\lambda_i}. \tag{26}$$

Therefore the final solution for $C(z,t)$ is given by

$$C(z,t) = \sum_{i=0}^{\infty} \frac{\sin(\lambda_i)}{\left(\frac{1}{2} - \frac{1}{4\lambda_i} \sin(2\lambda_i)\right)} \sin(\lambda_i z) e^{-\lambda_i^2 t}. \tag{27}$$

This series converges quickly as long as $t = O(1)$, as the terms decay exponentially. However for small t, the terms decay very slowly, and many terms need to be taken to ensure that the series has converged. To find the behaviour at small t, it is simpler to consider the small time asymptotic solution, which we derive in §4.

Points to note about this solution are:

- If $k = 0$, so that there is no re-uptake at the pre-synaptic membrane, then $\lambda_i = (2i+1)\pi/2$ and the solution (27) simplifies to

  $$C(z,t) = 2 \sum_{i=0}^{\infty} (-1)^i \sin(\lambda_i z) e^{-\lambda_i^2 t}. \tag{28}$$

  Parker [7] solved this using the method of images and obtained the solution

  $$C(z,t) = \frac{1}{\sqrt{\pi t}} \left(e^{-\frac{(1-z)^2}{4t}} + \sum_{i=1}^{\infty} \left(e^{-\frac{(1-z-2i)^2}{4t}} + e^{-\frac{(1-z+2i)^2}{4t}} \right) \right). \tag{29}$$

  Plotting (28) and (29) in Figure 5 for $t = 0.01$, we see that these two solutions are indistinguishable.

- At the other extreme $\kappa = \infty$, the solution does not work due to the incompatibility of the initial condition of a delta function release of particles and an infinite reuptake of particles at the presynaptic membrane (at $z = 0$). Parker [7] considered $\kappa = \infty$ with a source doublet (proportional to $\delta'(z-1)$) at $t = 0$. This initial condition is compatible and he was able to find a solution using the method of images.

- As $t \to \infty$, the leading-order current at the electrode is given by

$$I(t) \approx \frac{\lambda_0 \sin(\lambda_0)}{\left(\frac{1}{2} - \frac{1}{4\lambda_0}\sin(2\lambda_0)\right)} e^{-\lambda_0^2 t}. \tag{30}$$

  It is encouraging that the long-time decay observed in the experiments (cf. Figure 4) also appears to be exponential.

In Figure 6, we show how the concentration profile varies across the gap between the membrane and the electrode as time increases, assuming a mass transfer coefficient $\kappa = 10$. In Figure 7, we show how the electrode current $I(t)$ varies with t for different values of κ. We observe that each current profile has a peak, and in Figures 8 and 9, we plot how the size of the peak current and the time that it occurs change with the re-uptake rate κ. As expected we find that as κ increases, the peak current decreases since fewer particles reach the electrode due to the high re-uptake rate at the presynaptic membrane. The peak current also occurs sooner as κ increases. Finally we show in Figure 10 how the total charge Q collected by the electrode (equal to the integral of the current $I(t)$ for $0 \le t \le \infty$) varies with κ. Predictably it decreases as κ increases.

The current profiles in Figure 7 are remarkably similar to those observed in reality, such as that in Figure 4. By choosing the parameters C_0, D and k to make the model fit the current profiles, one can gain information about the total concentration of neurotransmitter released by a vesicle, its diffusion coefficient, and the rate of re-uptake by the pre-synaptic membrane. This will allow comparison of the process between snails of different ages or dosed with different drugs. We do not do the fitting in this report, but leave this for future work.

4 Small-time asymptotic solution to the 1D diffusion model

For small t we expect that the concentration has only spread a distance of $O(t^{1/2})$ from $z = 1$, and little material has had time to be re-adsorbed by the cell. Conservation of solute then implies that $C = O(t^{-1/2})$.

4.1 Transformation to similarity variables

Based on these expected scalings, we introduce similarity variable

$$\xi = \frac{1 - z}{\sqrt{4t}}\,, \tag{31}$$

and write

$$C(z,t) = \frac{1}{\sqrt{4t}} \mathscr{C}(\xi, t)\,. \tag{32}$$

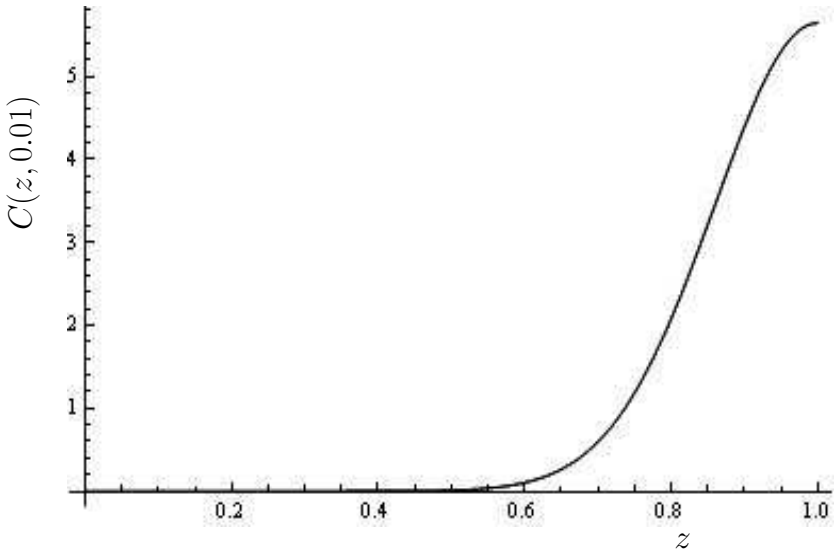

Figure 5: Plots of the separable solution (28) and Parker's [7] solution using the method of images (29) for $\kappa = 0$ at $t = 0.01$. The two solutions are indistinguishable.

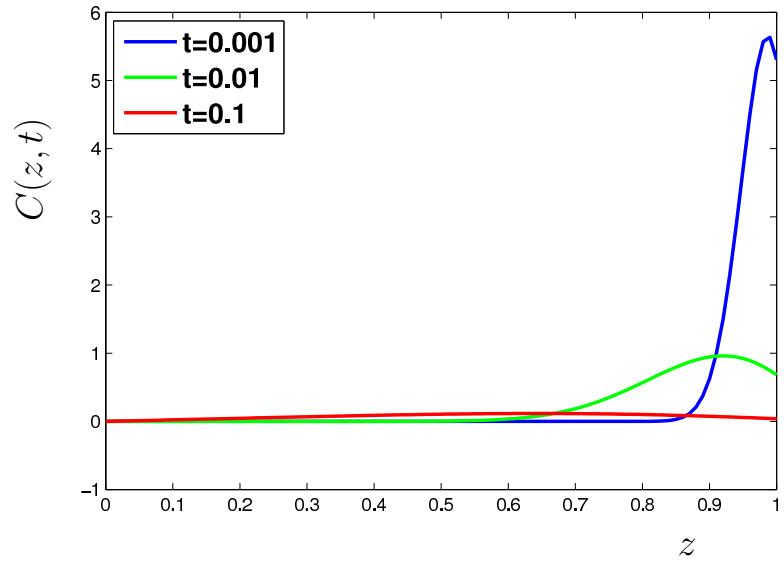

Figure 6: Variation of concentration $C(z, t)$ across the gap between the membrane and the electrode at different times for $\kappa = 10$.

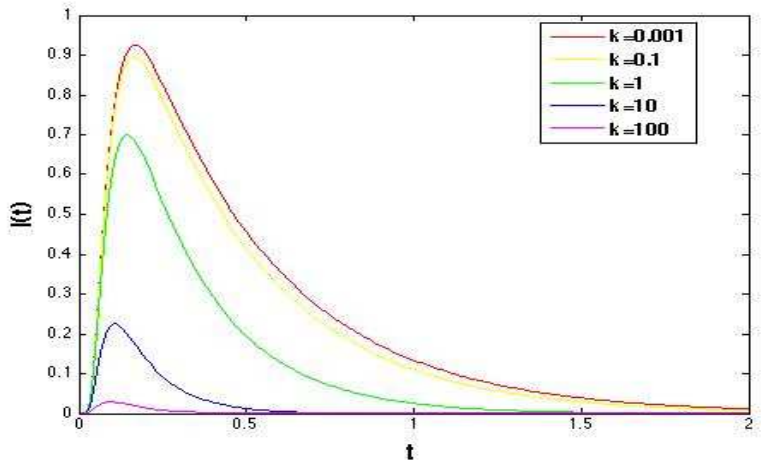

Figure 7: Variation of current $I(t)$ with t for increasing κ.

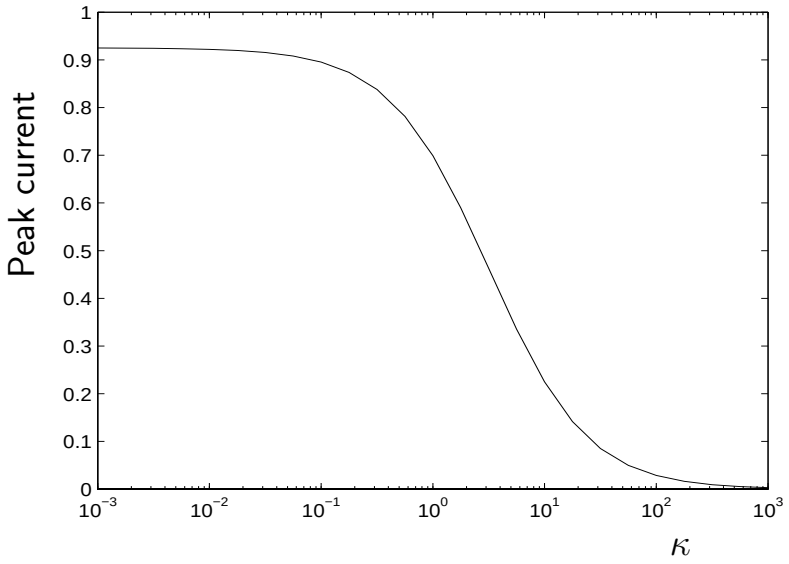

Figure 8: Variation of the peak current with the re-uptake rate κ.

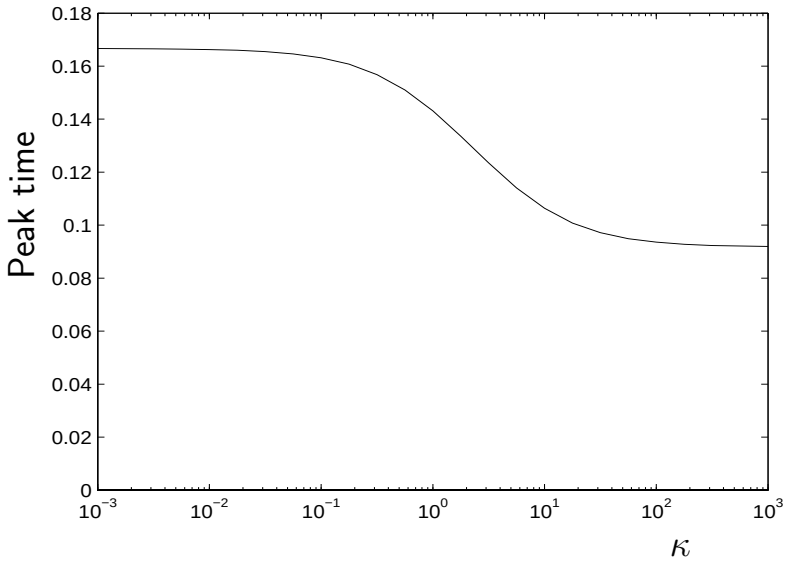

Figure 9: Variation of the time that the peak current occurs with the re-uptake rate κ.

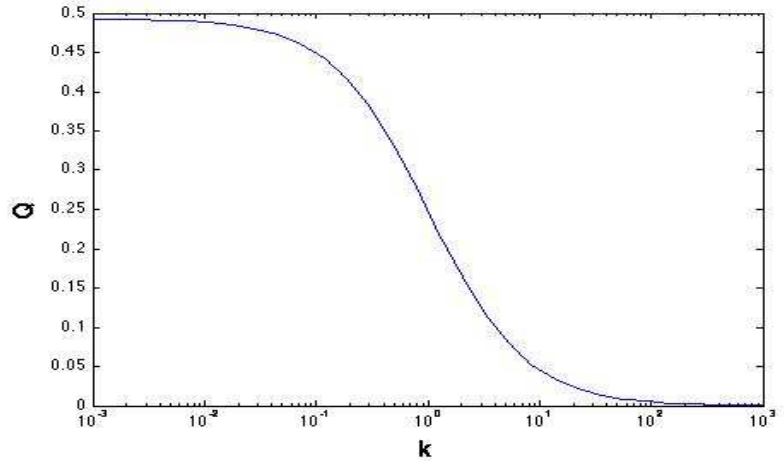

Figure 10: Variation of total charge Q detected by the electrode (equal to the integral of the current $I(t)$ for $0 \leq t \leq \infty$) with the re-uptake rate κ.

The diffusion equation (19) becomes

$$\frac{\partial^2 \mathscr{C}}{\partial \xi^2} + 2\xi \frac{\partial \mathscr{C}}{\partial \xi} + 2\mathscr{C} - 4t \frac{\partial \mathscr{C}}{\partial t} = 0\,, \tag{33}$$

while the boundary and initial conditions (20)–(22) become

$$\frac{\partial \mathscr{C}}{\partial \xi} = 2\kappa\, t^{1/2}\, \mathscr{C} \quad \text{on} \quad \xi = 0\,, \tag{34}$$

$$\mathscr{C} \to 0 \quad \text{as} \quad \xi \to \infty\,, \tag{35}$$

$$\int_0^\infty \mathscr{C}\, \mathrm{d}\xi = 1 \quad \text{as} \quad t \to 0\,. \tag{36}$$

4.2 Series expansion

To solve (33)–(36), we try a series expansion for $\mathscr{C}$ in powers of $\tau = 2\kappa t^{1/2}$:

$$\mathscr{C}(\xi, t) = \sum_{j=0}^{\infty} \tau^j \mathscr{C}_j(\xi) = \mathscr{C}_0(\xi) + \tau \mathscr{C}_1(\xi) + \tau^2 \mathscr{C}_2(\xi) + \ldots \tag{37}$$

We substitute the series into the equations and boundary conditions, and equate powers of τ.

For τ^0 we have:

$$\frac{\mathrm{d}^2 \mathscr{C}_0}{\mathrm{d}\xi^2} + 2\xi \frac{\mathrm{d}\mathscr{C}_0}{\mathrm{d}\xi} + 2\mathscr{C}_0 = 0\,, \tag{38}$$

subject to

$$\frac{\mathrm{d}\mathscr{C}_0}{\mathrm{d}\xi} = 0 \quad \text{on} \quad \xi = 0\,, \tag{39}$$

$$\mathscr{C}_0 \to 0 \quad \text{as} \quad \xi \to \infty\,, \tag{40}$$

$$\int_0^\infty \mathscr{C}_0\, \mathrm{d}\xi \;=\; 1\,. \tag{41}$$

For τ^j $(j > 0)$ we have

$$\frac{\mathrm{d}^2 \mathscr{C}_j}{\mathrm{d}\xi^2} + 2\xi \frac{\mathrm{d}\mathscr{C}_j}{\mathrm{d}\xi} + 2(1-j)\mathscr{C}_j = 0\,, \tag{42}$$

subject to

$$\frac{\mathrm{d}\mathscr{C}_j}{\mathrm{d}\xi} = \mathscr{C}_{j-1} \quad \text{on} \quad \xi = 0\,, \tag{43}$$

$$\mathscr{C}_j \to 0 \quad \text{as} \quad \xi \to \infty\,. \tag{44}$$

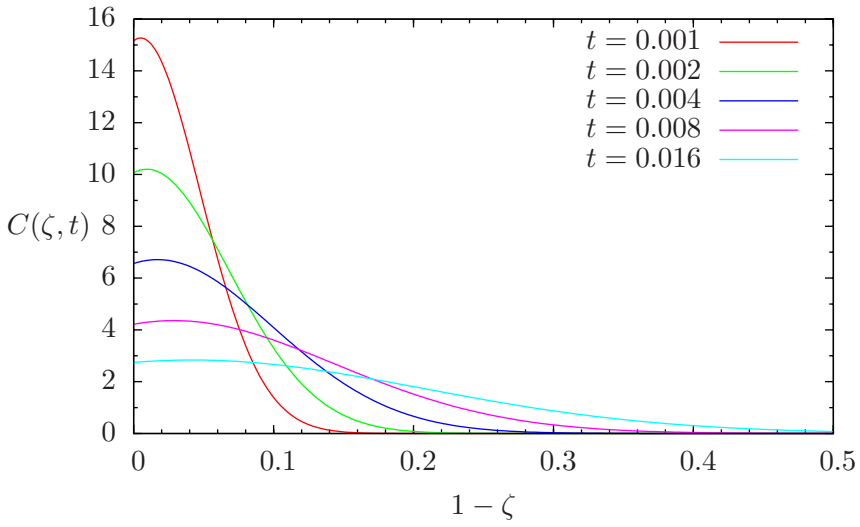

Figure 11: The evolution of the concentration profile at small times for $\kappa = 3$, using the first three terms in the series expansion (48).

4.3 Solution

Analytic solutions were obtained for the first three terms in the expansion:

$$\mathscr{C}_0(\xi) = \frac{2}{\sqrt{\pi}}\, e^{-\xi^2}\,, \tag{45}$$

$$\mathscr{C}_1(\xi) = -\operatorname{erfc}(\xi)\,, \tag{46}$$

$$\mathscr{C}_2(\xi) = \left(\frac{\mathrm{e}^{-\xi^2}}{\sqrt{\pi}} - \xi \operatorname{erfc}(\xi)\right)\,. \tag{47}$$

Observe that the solution for $\mathscr{C}_0$ is the standard Gaussian similarity solution for a point release next to an insulating boundary. The corrections are induced by the mixed boundary condition (34).

The solution for $C(z,t)$ is then given by

$$\begin{aligned} C(z,t) = {} & \frac{1}{\sqrt{\pi t}} \exp\left(-\frac{(1-z)^2}{4t}\right) - \kappa \operatorname{erfc}\left(\frac{1-z}{\sqrt{4t}}\right) \\ & + \kappa^2 \sqrt{4t}\left[\frac{1}{\sqrt{\pi}} \exp\left(-\frac{(1-z)^2}{4t}\right) - \frac{1-z}{\sqrt{4t}} \operatorname{erfc}\left(\frac{1-z}{\sqrt{4t}}\right)\right] + . \end{aligned} \tag{48}$$

Some typical curves are shown in Figure 11.

4.4 Validity

The series solution is only valid for small τ, so we require $t \ll \kappa^{-2}$. We must also ensure that the diffusive layer is confined near the cell, and has

not grown to approach the probe, since the $C = 0$ boundary condition at $z = 0$ is not satisfied exactly. This requires that the solution is confined within $1 - z \ll 1$, so we need $t \ll 1$.

Overall we expect this solution to be valid when

$$t \ll \min\{1, \kappa^{-2}\}\,. \tag{49}$$

4.5 Evaluating the current using the method of images

The current is given by the gradient of C at $z = 0$. The solution derived above does not satisfy the $C = 0$ boundary condition at $z = 0$ so cannot be used directly to estimate the concentration there. However, the method of images can be used to construct an approximate solution that does satisfy the boundary condition at $z = 0$, at the expense of not quite satisfying the condition at $z = 1$.

Writing

$$\tilde{C}(z,t) = C(z,t) + C(-z,t) \tag{50}$$

we see that $\tilde{C}(0,t) = 0$, and as long as $C(-1,t)$ is small (which it is for $t \ll 1$) then $\tilde{C}(1,t) \approx C(1,t)$ and the boundary condition at $z = 1$ is approximately satisfied.

Using $\tilde{C}(z,t)$ as an approximation for the solution near $z = 0$ we have that the current is given by

$$I = \left.\frac{\partial \tilde{C}}{\partial z}\right|_{z=0} = 2\left.\frac{\partial C}{\partial z}\right|_{z=0} \tag{51}$$

Using the first three terms from the series expansion, we obtain

$$I(t) = \frac{1}{2\sqrt{\pi t^3}} \exp\left(-\frac{1}{4t}\right) - \frac{\kappa}{\sqrt{\pi t}} \exp\left(-\frac{1}{4t}\right) + \kappa^2 \operatorname{erfc}\left(\frac{1}{\sqrt{4t}}\right) + \ldots \tag{52}$$

which we expect to be valid for $t \ll \min\{1, \kappa^{-2}\}$. Plots of $I(t)$ at small times are shown in Figure 12.

5 Boundary-layer problem for effective κ due to many discrete re-uptake sites

In this section we consider the effect of the re-adsorption at the cell occurring only at discrete uptake sites, rather than across the whole of the cell boundary. Specifically, we consider the case where there are a large number of small uptake sites, such that the (dimensional) size of the sites and the spacing between them are both $O(\delta L)$ where L is the gap width and $\delta << 1$. The uptake sites are assumed to be perfectly adsorbing ($\hat{C} = 0$) while the rest of the cell wall is insulating ($\partial \hat{C}/\partial z = 0$).

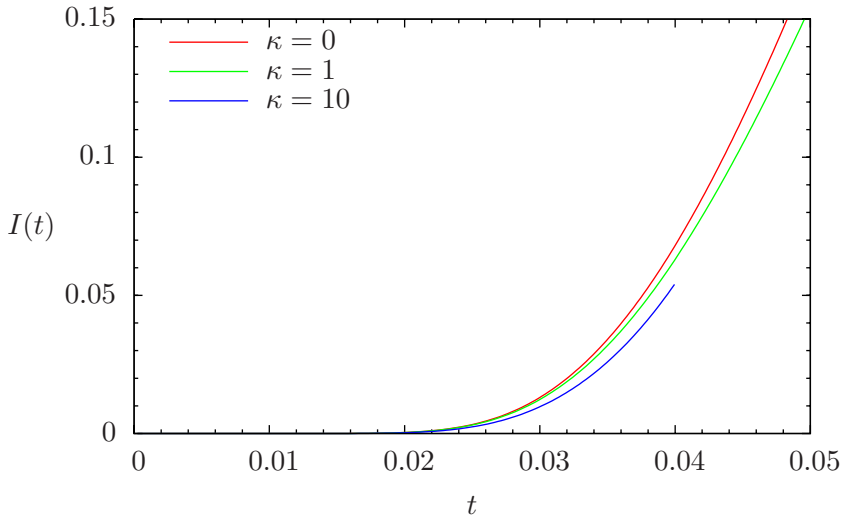

Figure 12: The evolution of the current at small times, using the first three terms in the series expansion (52).

5.1 Rescaling

Since $\delta \ll 1$ and the diffusion equation tends to produce equidimensional solutions, we expect the effect of the non-uniform boundary conditions to only be felt within a thin boundary layer of thickness δL next to the cell wall. We therefore rescale the non-dimensional spatial coordinates by a factor of δ. The time scale is still set by the outer problem in the bulk and so is unchanged. The concentration is expected to be small by a factor of δ, as the layer is thin, $\hat{C} = 0$ at some points on the cell wall, and fluxes need to be matched with those in the outer solution. We therefore write:

$$X = \frac{x}{\delta}\,, \qquad Y = \frac{y}{\delta}\,, \qquad Z = \frac{1-z}{\delta}\,, \qquad T = t\,, \qquad \mathscr{C} = \frac{\hat{C}}{\delta}\,. \tag{53}$$

With these variables, the diffusion equation becomes

$$\frac{\partial^2 \mathscr{C}}{\partial X^2} + \frac{\partial^2 \mathscr{C}}{\partial Y^2} + \frac{\partial^2 \mathscr{C}}{\partial Z^2} = 0\,, \tag{54}$$

since the time derivative is smaller by a factor of δ^2.

Boundary conditions are $\mathscr{C} = 0$ at the uptake sites, $\partial \mathscr{C}/\partial Z = 0$ on the rest of the cell. The inner limit of the outer solution is expected to satisfy a mixed boundary condition

$$\frac{\partial \hat{C}}{\partial z} + \kappa(x,y)\,\hat{C} = 0 \quad \Rightarrow \quad \hat{C} \sim A\left((1-z) + \frac{1}{\kappa(x,y)}\right) \quad \text{as} \quad z \to 1\,, \tag{55}$$

for some function $A(x,y)$.

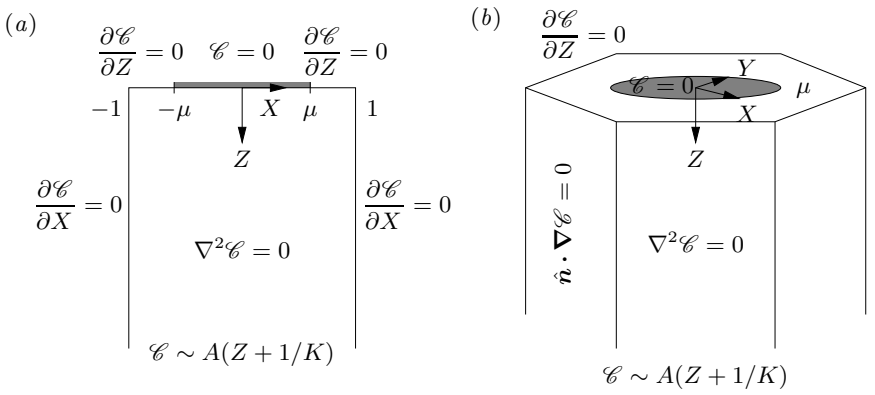

Figure 13: Unit cells for the boundary-layer problem of §5, in (a) a two-dimensional planar geometry, and (b) a three-dimensional hexagonal geometry.

Matching the inner and outer solutions we require

$$\mathscr{C} \sim A(\delta X, \delta Y) \left(Z + \frac{1}{K(\delta X, \delta Y)} \right) \quad \text{as} \quad Z \to \infty \tag{56}$$

where $K = \delta\kappa$.

From the solution in the inner boundary layer we should be able to find K, and hence the effective boundary condition on the outer concentration field.

5.2 A two-dimensional model problem

Consider a 2D problem in which the uptake sites have (non-dimensional) width $2\mu\delta$ and form a periodic array repeating every 2δ. We can then consider a unit cell problem, as depicted in Figure 13(a).

We need to solve

$$\nabla^2 \mathscr{C} = 0 \quad \text{in} \quad |X| < 1, \quad Z > 0\,, \tag{57}$$

subject to

$$\mathscr{C} = 0 \quad \text{on} \quad 0 <| X |< \mu, \quad Z = 0\,, \tag{58}$$

$$\frac{\partial \mathscr{C}}{\partial Z} = 0 \quad \text{on} \quad \mu <| X |< 1, \quad Z = 0\,, \tag{59}$$

$$\frac{\partial \mathscr{C}}{\partial X} = 0 \quad \text{on} \quad |X| = 1\,, \tag{60}$$

$$\frac{\partial \mathscr{C}}{\partial Z} \to A \quad \text{as} \quad Z \to \infty\,. \tag{61}$$

We can obtain an analytic solution to this problem using conformal transformations in the complex plane. We start with the upper half-plane out

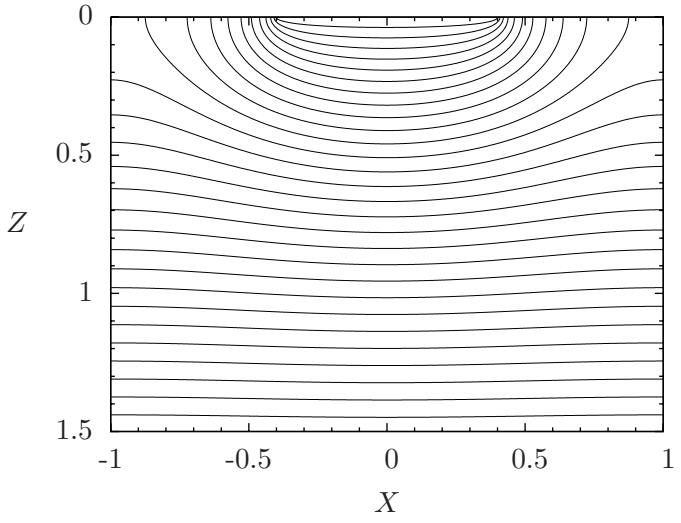

Figure 14: Equally spaced contours of $\mathscr{C}(X,Z)$ from (62) with $\mu = 0.4$ for the two-dimensional unit cell problem of §5.2.

side the unit circle, with $\mathscr{C} = 0$ on the circle and an insulating condition on the real axis. The solution here is then a multiple of $\log|w|$. We then apply a Joukowsky transform to flatten the circle, and a Schwarz–Christoffel mapping to fold up the real axis.

The solution is found to be given by

$$\mathscr{C}(X,Z) = \frac{2A}{\pi}\log\left|\frac{\sin(\frac{1}{2}\pi w)}{\sin(\frac{1}{2}\pi\mu)} + \sqrt{\frac{\sin^2(\frac{1}{2}\pi w)}{\sin^2(\frac{1}{2}\pi\mu)} - 1}\right| \tag{62}$$

where $w = X + \mathrm{i}Z$. From this solution, we find

$$\mathscr{C}(X,Z) \sim A\left(Z - \frac{2}{\pi}\log\left|\sin(\tfrac{1}{2}\pi\mu)\right|\right) \quad \text{as} \quad Z \to \infty\,. \tag{63}$$

We therefore have

$$K = -\frac{\pi}{2\log\left|\sin(\frac{1}{2}\pi\mu)\right|}\,. \tag{64}$$

A typical contour plot for $\mathscr{C}(X,Z)$ is shown in Figure 14, and the limting vertical concentration profiles are shown in Figure 15. A plot of the dependence of κ on μ is shown in Figure 16. Observe that μ must be fairly small to obtain $\kappa \le O(1)$ (especially when δ is small). So unless the uptake sites are sufficiently small, we will obtain an effective boundary condition of perfect re-adsorption ($\hat{C} \approx 0$) at the cell.

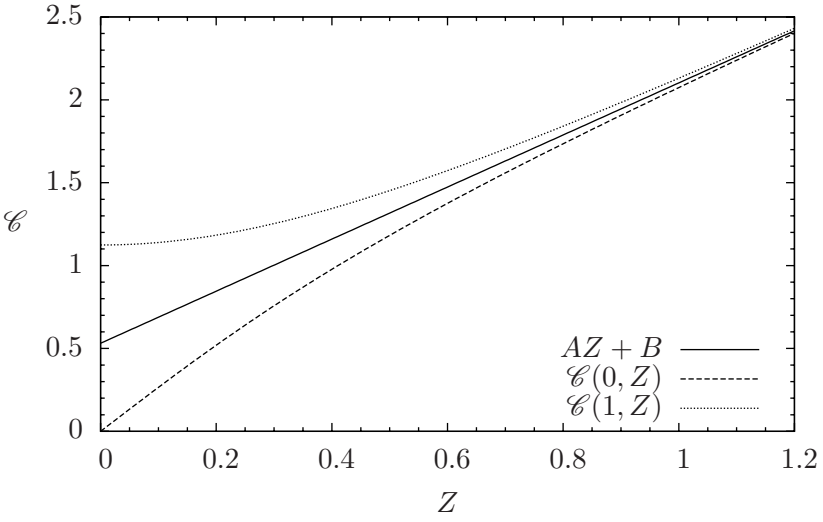

Figure 15: Concentration profiles (62) for the two-dimensional unit cell problem of §5.2. We show the limiting profiles at $X = 0$ and $X = 1$ and the asymptotic linear function $AZ + B$ for $\mu = 0.4$.

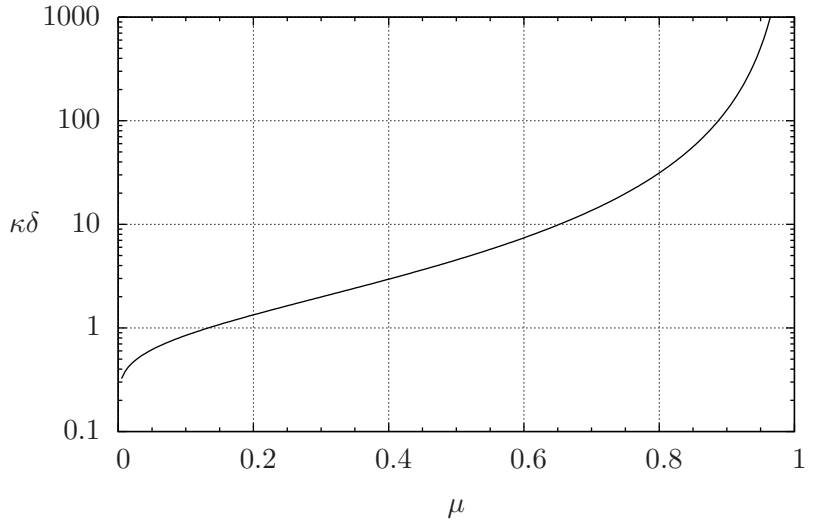

Figure 16: The effective boundary constant κ as a function of the fraction μ of uptake sites (64) for the two-dimensional problem.

5.3 A three-dimensional model problem

In 3D, we could consider a hexagonal array of circular uptake sites. The domain and boundary conditions for the unit cell would then be as depicted in Figure 13(b). Conformal mappings can no longer be used here, and we would have to resort to numerical solution of Laplace's equation.

6 Numerical investigation of the effect of discrete re-uptake sites

In this section, we consider the effect of discrete re-uptake sites by simulating the problem numerically in the commercial software package COMSOL Multiphysics. Firstly however in §6.1, in order to validate the numerical method, we consider the 1D diffusion problem with uniform re-uptake presented in §2.2 and compare the numerical solution with the analytical results to ensure that they are comparable. Then in §6.2, we consider a 2D diffusion model containing a single release site and a single re-uptake site. Both sites are assumed to be the same size and separated by a distance d, and we assume that flux through the re-uptake site is proportional to the concentration using a mass transfer coefficient κ. We investigate the impact of varying d and κ.

6.1 1D diffusion model with one release site and uniform re-uptake across the membrane

Firstly we set up COMSOL Multiphysics to solve the problem with one release site and uniform re-uptake across the membrane, described in §2.2, with governing equation and boundary and initial conditions given by (19)-(22). The domain is modelled by a rectangular shape with $-0.1 \leq x \leq 0.1$ and $0 \leq z \leq 1$, where as before the upper edge at $z = 1$ is the presynaptic membrane and the lower edge at $z = 0$ represents the electrode. The boundary conditions on the upper and lower edges are the same as (20) and (21). The boundary conditions on the vertical edges assume no flux as we are considering a one-dimensional model where the diffusion occurs only in the vertical direction. Analytically we modelled the instantaneous particle release as a δ-Dirac function, cf. (22). This is difficult to implement in Comsol, so we approximated it by using the function flc2hs, which is a smoothed Heaviside function, so that the particles are located near the membrane at $t = 0$. Thus we can summarize the problem for $C(x, z, t)$ as follows:

Governing equation:

$$\frac{\partial C}{\partial t} = \nabla^2 C \tag{65}$$

Initial condition at $t = 0$:

$$C(x, z, t) = 26\,\mathsf{flc2hs}(\mathsf{z} - 1, 0.13), \text{ for } 0 \leq \mathsf{z} \leq 1. \tag{66}$$

Boundary conditions for $t > 0$:

$$C(x, 0, t) = 0, \tag{67}$$

$$-\frac{\partial C}{\partial z}(x, 1, t) = \kappa C(x, 1, t), \tag{68}$$

$$\frac{\partial C}{\partial x} = 0 \quad \text{at } x = -0.1, x = 0.1. \tag{69}$$

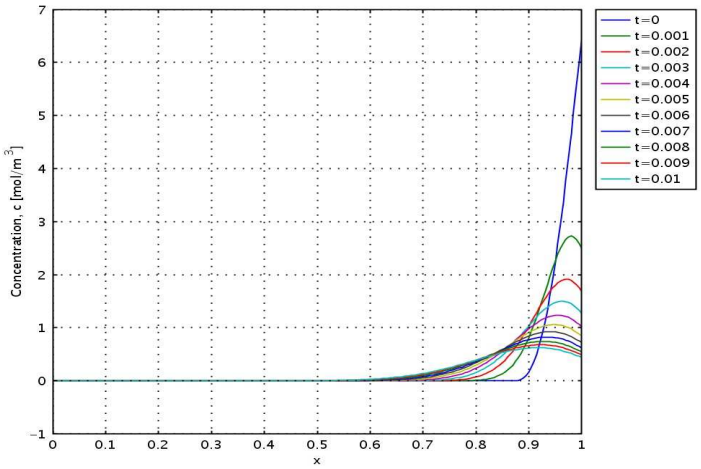

Figure 17: Concentration of neurotransmitter in the gap between the membrane and the electrode with $\kappa = 10$ for different values of time.

In Figure 17 we show how the numerical solution for the concentration varies with time for mass transfer coefficient $\kappa = 10$. The total amount of neurotransmitter decreases when $t = O(10^{-3})$ due to re-uptake into the membrane, and the concentration peak decreases as the neurotransmitter diffuses across to the electrode. These results are consistent with the analytical solution plotted in Figure 6, and give us confidence in the numerical model.

6.2 2D diffusion model with a single release site and a single re-uptake site

In reality the re-uptake of neurotransmitters does not take place uniformly across the cell membrane, but only at certain locations. Modelling this effect

might lead to a better understanding of the measured data. We again used a rectangle of height $0 \leq z \leq 1$, but with width $-25 \leq x \leq 25$, the width being significantly longer than the height as the length of the electrode and the membrane are treated as being infinite. At the vertical boundaries we set no flux boundary conditions as we assume that none of the neurotransmitter escapes out the sides of the electrode. To take into account discrete release and re-uptake sites on the membrane, we separate the upper edge of the rectangle into five intervals $I_j,\ j = 1, .., 5$, where I_2 represents the site of release (i.e. initially the particles are present only near this interval) and I_4 the place of re-uptake. The distance d between I_2 and I_4 has an important influence on the concentration profile and we vary it to see how it affects the current detected at the electrode. For $t > 0$, the boundary condition at I_4 is equal to (21) with mass transfer coefficient κ, while at the other four intervals no-flux conditions are set. We assume that the release and the re-uptake sites are the same length, namely 1/200 times the distance between the membrane and the electrode. The 2D-problem is therefore stated as:

Governing equation:

$$\frac{\partial C}{\partial t} = \nabla^2 C \tag{70}$$

Initial condition, at $t = 0$:

$$C(x, z, 0) = 26\,\mathsf{flc2hs}(\mathsf{z} - 1, 0.13), \quad \text{for } \mathsf{x} \in \mathsf{I}_2,\ 0 \leq \mathsf{z} \leq 1, \tag{71}$$

$$C(x, z, 0) = 0, \quad \text{for } x \notin I_2,\ 0 \leq z \leq 1. \tag{72}$$

Boundary conditions for $t > 0$:

$$\frac{\partial C}{\partial z}(x, 1, t) = 0, \quad \text{at } x \in I_1, I_2, I_3, I_5, \tag{73}$$

$$-\frac{\partial C}{\partial z}(x, 1, t) = \kappa\, C(x, 1, t), \quad \text{at } x \in I_4, \tag{74}$$

$$C(x, 0, t) = 0, \tag{75}$$

$$\frac{\partial C}{\partial x}(x, z, t) = 0, \quad \text{at } x = -25 \text{ and } x = 25. \tag{76}$$

The current generated at the electrode is calculated as follows:

$$I(t) = \int_{-25}^{25} \frac{\partial C}{\partial z}(x, 0, t)dx. \tag{77}$$

For illustration, we chose the following intervals on the membrane at

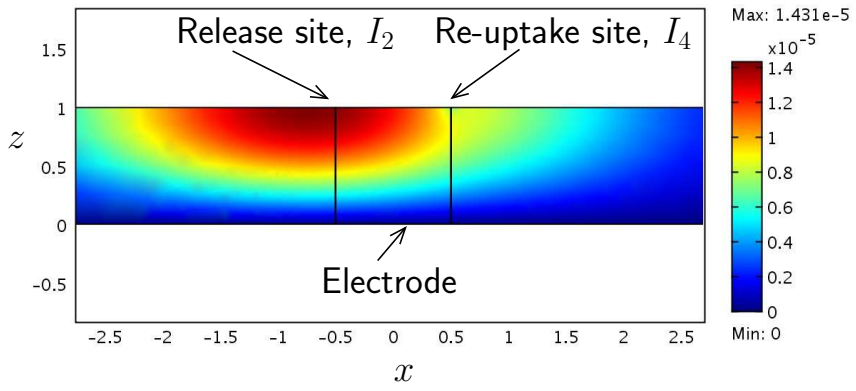

Figure 18: Concentration of neurotransmitter in the gap between the membrane and the electrode after two seconds with mass transfer coefficient at the re-uptake site $\kappa = 100$. On the membrane at $z = 1$, the release site is at $I_2 : -0.505 \leq x \leq 0.5$, and the re-uptake site is at $I_4 : 0.5 \leq x \leq 0.505$, so that the distance between them is $d = 1$.

$z = 1$:

$$I_1 : -25 \leq x \leq -0.505, \tag{78}$$
$$I_2 : -0.505 \leq x \leq 0.5, \text{ (the release site)}, \tag{79}$$
$$I_3 : -0.5 \leq x \leq 0.5, \tag{80}$$
$$I_4 : 0.5 \leq x \leq 0.505, \text{ (the re-uptake site)}, \tag{81}$$
$$I_5 : 0.505 \leq x \leq 25, \tag{82}$$

so that the distance between the release site and the re-uptake site is $d = 1$. In Figure 18 we show the distribution of concentration with $\kappa = 100$ after two seconds. We notice how the neurotransmitter has diffused more on the lefthand side, where the releasing site is located, than on the right side, where the re-uptake site is located.

Figure 19 shows how the current $I(t)$ varies at the electrode with time and the different lines correspond to different values of κ. The distance between the sites is $d = 0.1$. As expected the current decreases with increasing κ. We only obtained a significant difference in $I(t)$ after $t = 2$ if the distance between the release and the re-uptake sites is small.

In Figure 20 we show how the value of d affects the current $I(t)$ for $\kappa = 100$. Increasing d causes the maximum value of $I(t)$ to increase, as

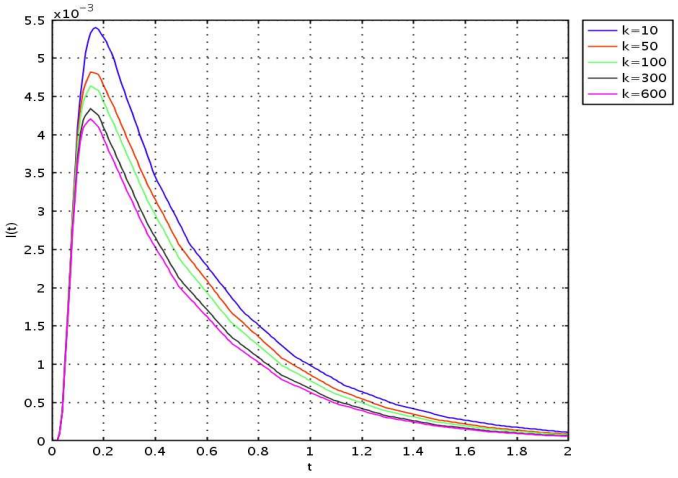

Figure 19: Graph of how the current $I(t)$ varies for different values of the mass transfer coefficient κ. The distance between the release and re-uptake sites is $d = 0.1$.

for larger d the neurotransmitters have not had time to diffuse close to the re-uptake site. For $d \geq 0.2$ the peaks in the profile are indistinguishable, but these current profiles become distinguishable at longer times, when the neurotransmitters begin to reach the re-uptake site. Lines with $d \geq 2$ are still close for times close to $t = 2$, since the neurotransmitter still has not reached the re-uptake site.

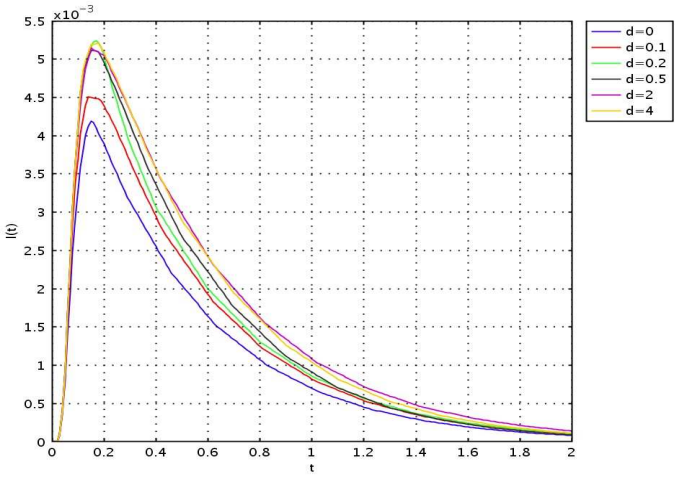

Figure 20: Graph of how the current $I(t)$ varies as the distance d between the release and re-uptake sites changes. The mass transfer coefficient $\kappa = 100$.

In summary, we have seen that the 1D numerical simulation compares well with the results found by solving the problem analytically. In the 2D case with discrete release and re-uptake sites, the simulations show the results that one would expect: the larger the distance d between the release and the re-uptake sites, the fewer particles are absorbed and consequently more particles reach the electrode, whereas with increasing re-uptake rate κ more neurotransmitters are absorbed and less current is recorded on the electrode. To obtain a more quantitative description of these dependencies one would have to consider a variety of settings with different d/κ-combinations.

7 Conclusions and future work

Neurotransmitter molecules are released from a vesicle through the presynaptic membrane, and subsequently diffuse away, although some are reabsorbed by the membrane. Questions to be answered about this process include how it changes with age and drugs. The neurotransmitter molecules from a single vesicle release can be detected using a microelectrode. Once they strike the surface of the electrode, they are oxidised and produce a current. By analysing the profile of this current over time, experimentalists would like to be able to deduce features of the process, such as the total amount of neurotransmitter released and the re-uptake rate into the membrane.

Assuming that the release of the neurotransmitter is instantaneous and from a point (cf. [7]), we have derived a simple model for the process. The other key assumptions are firstly that the re-uptake takes place uniformly across the membrane and may be represented by a constant mass transfer coefficient k; secondly, that the rate of oxidation at the electrode is so fast that the concentration of neurotransmitter is zero there; and thirdly, that the gap between the electrode and the membrane surface is much smaller than the diameter of the electrode so that the membrane and the electrode can be modelled as two planes. This model may be solved as a series solution, and the current profiles that it generates are very similar to those observed experimentally, in particular the exponential decay for large time. For small time, the series solution requires a large number of terms to converge, and at these times it is more practical to find the asymptotic solution. We have found the first three terms in this series and shown how it is possible to use the method of images to approximate the current.

A major assumption in the model described in the previous paragraph is the uniform re-uptake across the membrane. In reality the re-uptake takes place at discrete sites. If there are a large number of perfectly absorbing sites, whose size and separation is small compared to the distance between the electrode and the membrane and distributed periodically across the membrane, then all the non-uniformity caused by their distribution is

contained in a small boundary layer near the membrane and by solving the problem in this boundary layer we have shown how to deduce the effective mass transfer coefficient due to these sites. In addition to this analytical approach, we have done some preliminary numerical investigations into the effect of a single re-uptake site on the current experienced by the electrode, assuming that the re-uptake site and the vesicle release site are of similar size. In particular we have investigated the effect of changing the distance of separation of the two sites, and also changing the mass transfer coefficient in the re-uptake site. The effects are as would be expected, but further work is needed to quantify precisely the effects over the whole parameter space.

7.1 Further work

Suggestions for further work include:

- Fitting of the simple model solution for the current profile to various vesicle releases from snails of different ages or subjected to different drugs to see if the fitted parameters give realistic answers, and to see if any deductions can be made about the effect of the aging process or drugs on the neurotransmitter release process;
- Use the boundary layer approach to estimate an effective mass transfer parameter for a particular membrane;
- Perform more numerical work on the effect of a single re-uptake site on the current measured at the electrode to quantify precisely the effects of distance from the release site and mass transfer coefficient.
- Collaborate with the biologists and experimentalists to make sure that our models are appropriate and to agree on future directions for the modelling. For instance, it would be useful to have more detail on the configuration and nature of the re-uptake sites and more detail about the release mechanism.

References

[1] Wightman R.M., Haynes C.L., *Nature Neuroscience*, **2004**, *7:4*, 321-322.

[2] Wightman R.M., Schroeder T.J., Finnegan J.M., Ciolkowski E.L., Pihel K., Time course of release of catecholamines from individual vesicles during exocytosis at adrenal medullary cells, *Biophysical Journal*, **1995**, *68*, 383-390.

[3] Sombers L.A., Hanchar H.J., Colliver T.L., Wittenberg N., Cans A., Arbault S., Amatore C., Ewing A.G., The effects of vesicular volume

on secretion through the fusion pore in exocytotic release from PC12 cells, *The Journal of Neuroscience*, **2004**, *24(2)*, 303-309.

[4] Amatore C., Arbault S., Bonifas I., Bouret Y., Erard M., Ewing A.G., Sombers L.A., Correlation between vesicle quantal size and fusion pore release in chromaffin cell exocytosis, *Biophysical Journal*, **2005**, *88*, 4411-4420.

[5] Wu, W-Z., Huang W-H., Wang W., Wang Z-L., Cheng J-K., Xu T., Zhang R-Y., Chen Y., Liu J., Monitoring dopamine release from single living vesicles with nanoelectrodes, *Journal of the American Chemical Society*, **2005**, *127*, 8914-8915.

[6] Rabie H.R., Rong J., Glavinovic M.I., Monte Carlo simulation of release of vesicular content in neuroendocrine cells, *Biological Cybernetics*, **2006**, *94*, 483-499.

[7] Parker K.H., Some thoughts on the electrode signal due to the release of neurotransmitters, **2006**, *Private communication.*